Synthesis of Nickel−Nitrilotriacetic Acid Coupled Single-Walled Carbon Nanotubes for Directed Self-Assembly with Polyhistidine-Tagged Proteins

Rachel A. Graff, Thomas M. Swanson, and Michael S. Strano*

Department of Chemical Engineering, Massachusetts Institute of Technology, 77 Massachusetts Avenue, Cambridge, Massachusetts 02139

Received September 11, 2007

Nickel−nitrilotriacetic acid-functionalized single-walled carbon nanotubes have been synthesized for the directed, reversible self-assembly of polyhistidine-tagged macromolecules onto the nanotube surface. Carbon nanotubes were first covalently functionalized with 4-carboxybenzene diazonium salt, which rendered them water-soluble. The acid moieties on the carbon nanotube were covalently reacted with N_α,N_α-bis(carboxymethyl)-L-lysine hydrate, forming amide bonds to the nanotube complex. The nitrilotriacetic acid (NTA) moiety of the N_α,N_α-bis(carboxymethyl)-L-lysine was complexed with Ni^{2+} and used to specifically bind a polyhistidine-tagged photosynthetic reaction center (RC) from *Rhodobacter sphaeroides* as a model system. We demonstrate that the histidine-tagged RC protein (RC-His) specifically binds to SWNT-NTA-Ni in a reversible manner. The free RC-His in solution can be removed through histidine binding to Ni-NTA-agarose resin and purified by filtration. This approach allows for both positional and orientational control over protein binding to carbon nanotubes.

Introduction

Carbon nanotubes are of interest as components of nanoscale self-assembled multifunctional materials, particularly for electronics, optoelectronics, and photovoltaic applications.[1–4] They have high electrical conductivity,[5] high tensile strength,[6] and unique optical properties that are sensitive to their environment.[7–9] Single-walled carbon nanotubes (SWNT) contain a mixture of semiconducting and metallic structures depending on the diameter and chirality of the nanotube and are ideal for use as molecular wires in self-assembled systems.[10] They are not easily dispersed in solution due to their hydrophobicity and strong van der Waals intertube interaction, which align the tubes into roped aggregates.[11,12] Bundles of semiconducting and metallic nanotubes act primarily as metal aggregates.[13,14]

Many techniques exist for suspending SWNT individually in solution, either with surfactant stabilization and ultrasonication or by covalent functionalization of the nanotube with a soluble ligand.[15–17] Solvent compatibility is a key issue for directing the self-assembly of a protein onto a nanotube, as all processing should be in aqueous solution under conditions that do not denature the protein. It is a challenge to direct the assembly of the protein onto the sidewall of the suspended nanotube with controlled orientation. The protein either can be directly adsorbed onto the carbon nanotube sidewall or can be attached near the surface with a chemical linker.[18–22] When a protein is adsorbed onto the surface of a hydrophobic carbon nanotube, there can be some changes in its structure which can result in a loss of protein activity.[18] Not all proteins are denatured by the hydrophobic interaction with the carbon nanotube system. Glucose oxidase

* Corresponding author. E-mail: strano@mit.edu.

(1) Bandaru, P. R. *J. Nanosci. Nanotechnol.* **2007**, *7*, 1239–1267.
(2) Mahar, B.; Laslau, C.; Yip, R.; Sun, Y. *IEEE Sens. J.* **2007**, *7*, 266–284.
(3) Trojanowicz, M. *TrAC, Trends Anal. Chem.* **2006**, *25*, 480–489.
(4) Avouris, P. *Acc. Chem. Res.* **2002**, *35*, 1026–1034.
(5) Hamada, N.; Sawada, S.; Oshiyama, A. *Phys. Rev. Lett.* **1992**, *68*, 1579–1581.
(6) Bernholc, J.; Brenner, D.; Nardelli, M. B.; Meunier, V.; Roland, C. *Annu. Rev. Mater. Res.* **2002**, *32*, 347–375.
(7) Weisman, R. B.; Bachilo, S. M.; Tsyboulski, D. *Appl. Phys. A* **2004**, *78*, 1111–1116.
(8) Saito, R.; Gruneis, A.; Samsonidze, G. G.; Dresselhaus, G.; Dresselhaus, M. S.; Jorio, A.; Cancado, L. G.; Pimenta, M. A.; Souza, A. G. *Appl. Phys. A* **2004**, *78*, 1099–1105.
(9) Lefebvre, J.; Fraser, J. M.; Homma, Y.; Finnie, P. *Appl. Phys. A* **2004**, *78*, 1107–1110.
(10) Nygard, J.; Cobden, D. H.; Bockrath, M.; McEuen, P. L.; Lindelof, P. E. *Appl. Phys. A* **1999**, *69*, 297–304.
(11) Thess, A.; Lee, R.; Nikolaev, P.; Dai, H. J.; Petit, P.; Robert, J.; Xu, C. H.; Lee, Y. H.; Kim, S. G.; Rinzler, A. G.; Colbert, D. T.; Scuseria, G. E.; Tomanek, D.; Fischer, J. E.; Smalley, R. E. *Science* **1996**, *273*, 483–487.
(12) Girifalco, L. A.; Hodak, M.; Lee, R. S. *Phys. Rev. B* **2000**, *62*, 13104–13110.
(13) Okada, S.; Oshiyama, A.; Saito, S. *Phys. Rev. B* **2000**, *62*, 7634–7638.
(14) Lacerda, L.; Pastorin, G.; Wu, W.; Prato, M.; Bianco, A.; Kostarelos, K. *Adv. Funct. Mater.* **2006**, *16*, 1839–1846.
(15) Fu, K. F.; Sun, Y. P. *J. Nanosci. Nanotechnol.* **2003**, *3*, 351–364.
(16) Matarredona, O.; Rhoads, H.; Li, Z. R.; Harwell, J. H.; Balzano, L.; Resasco, D. E. *J. Phys. Chem. B* **2003**, *107*, 13357–13367.
(17) Hilding, J.; Grulke, E. A.; Zhang, Z. G.; Lockwood, F. *J. Dispersion Sci. Technol.* **2003**, *24*, 1–41.
(18) Karajanagi, S. S.; Vertegel, A. A.; Kane, R. S.; Dordick, J. S. *Langmuir* **2004**, *20*, 11594–11599.
(19) Barone, P. W.; Baik, S.; Heller, D. A.; Strano, M. S. *Nat. Mater.* **2005**, *4*, 86–92.
(20) Chen, R. J.; Bangsaruntip, S.; Drouvalakis, K. A.; Kam, N. W. S.; Shim, M.; Li, Y. M.; Kim, W.; Utz, P. J.; Dai, H. J. *Proc. Natl. Acad. Sci. U.S.A.* **2003**, *100*, 4984–4989.
(21) Yu, X.; Chattopadhyay, D.; Galeska, I.; Papadimitrakopoulos, F.; Rusling, J. F. *Electrochem. Commun.* **2003**, *5*, 408–411.
(22) Liu, J. Q.; Chou, A.; Rahmat, W.; Paddon-Row, M. N.; Gooding, J. J. *Electroanalysis* **2005**, *17*, 38–46.

10.1021/cm702577h CCC: $40.75
Published on Web 02/19/2008

and soybean peroxidase retain significant activity on the nanotube surface, while α-chymotrypsin is rendered inactive.[18,19] Coupling a carbon nanotube with a protein via a chemical linker can help retain protein activity. The chemical linker can either have a moiety which acts as a binding site for the protein of interest or covalently react with amines on the protein surface. Tween has been successfully functionalized with SpA, which specifically binds to IgG antibodies.[20] When nanotubes are suspended noncovalently with Tween−SpA, the surface coverage prevents nonspecific adsorption of proteins onto the surface, targeting only IgG. In that study Tween was also biotinylated to direct assembly of streptavidin onto the nanotube surface. This assembly technique depends on using binding partners with high specificity. For covalent binding of proteins, amide bonds have been formed between various proteins (glucose oxidase, flavin adenine dinucleotide, and iron heme enzymes) and acid-functionalized nanotubes through nucleophilic substitution.[21,22] This reaction will direct most proteins to the surface of the nanotube, but it does not control the orientation of the protein on the nanotube surface.

The goal of this work is to use covalent functionalization of the nanotube sidewall to bind proteins at controlled orientation while maintaining activity of the attached protein. The key to this assembly is to have a linker on the protein that will recognize the functional groups on the nanotube. The high binding affinity for histidine amino acid to nickel is of particular interest. For recombinant proteins a polyhistidine tag (~6 histidine residues in a chain) can be expressed on the C- or H-terminus of the protein as this sequence allows for efficient complexation with nickel as long as the histidine is not deprotonated (pH < 5).[23] This tag is often used for the purification of recombinant protein using a nickel-chelated column where the nickel is immobilized onto a *N*-(5-amino-1-carboxypentyl)iminodiacetic acid (NTA)-functionalized resin.[23,24] This binding can be reversed by the addition of imidazole (150–300 mM). The approach used in this work is to use an NTA derivative to react with carboxylic acid-functionalized nanotubes. The NTA ligand is complexed with nickel and recombinant proteins directly bind to the functionalized nanotube at controlled orientation dependent on the location of the polyHis tag. Previously nanotubes have been suspended with NTA-functionalized lipids which were noncovalently adsorbed to the nanotube sidewall.[25] Although this suspension was successful, excess lipid remains in equilibrium in solution, resulting in binding sites for the recombinant protein that are not directly on the surface of the nanotube.

The model protein used for this study was a photosynthetic reaction center (RC) from purple non-sulfur bacterium, *Rhodobacter sphaeroides*.[26,27] This protein complex is of particular interest for the development of novel photovoltaic complexes that can make electronic contact with the photoactive components of the RC structure.[28–33] This requires controlled orientation of the protein during self-assembly because the donor dimer (P870) is located on a hydrophilic region of the RC which will not orient toward the carbon nanotube (potential electron donor) through direct adsorption. The RC used in this study was designed to express a polyhistidine tag on the C-terminal of the M subunit close to the primary donor dimer (P870), which ideally should allow for orientation toward the carbon nanotube when the His tag binds to the functionalized nanotube. RC is a pigment–protein complex with unique absorption signatures that fluoresce in the near-infrared and can be used to image protein binding to functionalized carbon nanotubes.

Here we report the covalent functionalization of single-walled carbon nanotubes with a nitrilotriacetic ligand that can complex nickel for directing the reversible self-assembly of polyhistidine tagged proteins onto the nanotube surface at controlled orientation (Scheme 1).

Experimental Section

Materials. All materials and chemicals were purchased from Aldrich unless otherwise stated. AP-SWNT (as-prepared) material was purchased from Carbon Solutions, Inc., synthesized by electric arc discharge. AP-SWNT have an average diameter of 1.4 nm and a length range of 0.5–3 μm. They were suspended in 1% sodium dodecyl sulfate in DI water (1 mg/mL), probe-tip sonicated 1 h (5 W), and centrifuged at 30 000 rpm for 1 h to isolate individual species. Dialysis tubing was purchased from Pierce with molecular weight cutoffs (MWCO) of 10 000 and 12 000–14 000 g/mol. Polyhistidine-tagged reaction centers (RC) from *Rhodobacter sphaeroides* were obtained from the laboratory of C. A. Wraight, Department of Biochemistry at the University of Illinois at Urbana–Champaign. Nickel-NTA-agarose resin was purchased from Qiagen with a binding capacity of 5–10 mg/mL.

4-Carboxybenzene Diazonium Tetrafluoroborate. 4-Carboxybenzene diazonium tetrafluoroborate salt was synthesized following previous methods[34,35] using a 4-aminobenzoic acid precursor. The synthesis of the desired diazonium salt was confirmed with ^{1}H NMR (400 MHz, CD_3CN) δ 8.41, 8.55 ppm (CH_2, s, 2H) and high-resolution mass spectroscopy with electrospray ionization, *m*/*z* 149 ($C_7H_5N_2O_2^+$).

SWNT-COOH. The individually suspended AP-SWNT were reacted twice with 4-carboxybenzene diazonium salt dissolved in a 1% SDS solution in deionized water to attach an carboxyphenyl moiety to the nanotube. The nanotubes were first reacted with 3

(23) Ueda, E. K. M.; Gout, P. W.; Morganti, L. *J. Chromatogr., A* **2003**, *988*, 1–23.
(24) Hochuli, E.; Dobeli, H.; Schacher, A. *J. Chromatogr.* **1987**, *411*, 177–184.
(25) Richard, C.; Balavoine, F.; Schultz, P.; Ebbesen, T. W.; Mioskowski, C. *Science* **2003**, *300*, 775–778.
(26) Camara-Artigas, A.; Brune, D.; Allen, J. P. *Proc. Natl. Acad. Sci. U.S.A.* **2002**, *99*, 11055–11060.
(27) Giardi, M. T.; Pace, E. *Trends Biotechnol.* **2005**, *23*, 257–263.
(28) Lebedev, N.; Trammell, S. A.; Spano, A.; Lukashev, E.; Griva, I.; Schnur, J. *J. Am. Chem. Soc.* **2006**, *128*, 12044–12045.
(29) Noy, D.; Moser, C. C.; Dutton, P. L. *Biochim. Biophys. Acta* **2006**, *1757*, 90–105.
(30) Frolov, L.; Rosenwaks, Y.; Carmeli, C.; Carmeli, I. *Adv. Mater.* **2005**, *17*, 2434–2437.
(31) Nakamura, C.; Hasegawa, M.; Yasuda, Y.; Miyake, J. *Appl. Biochem. Biotechnol.* **2000**, *84–6*, 401–408.
(32) Lu, Y. D.; Yuan, M. J.; Liu, Y.; Tu, B.; Xu, C. H.; Liu, B. H.; Zhao, D. Y.; Kong, J. L. *Langmuir* **2005**, *21*, 4071–4076.
(33) Das, R.; Kiley, P. J.; Segal, M.; Norville, J.; Yu, A. A.; Wang, L. Y.; Trammell, S. A.; Reddick, L. E.; Kumar, R.; Stellacci, F.; Lebedev, N.; Schnur, J.; Bruce, B. D.; Zhang, S. G.; Baldo, M. *Nano Lett.* **2004**, *4*, 1079–1083.
(34) Nair, N.; Kim, W. J.; Usrey, M. L.; Strano, M. S. *J. Am. Chem. Soc.* **2007**, *129*, 3946–3954.
(35) Strano, M. S.; Dyke, C. A.; Usrey, M. L.; Barone, P. W.; Allen, M. J.; Shan, H. W.; Kittrell, C.; Hauge, R. H.; Tour, J. M.; Smalley, R. E. *Science* **2003**, *301*, 1519–1522.

Scheme 1. Reaction Scheme for the Nickel Functionalization of SWNT following Reaction with 4-Carboxybenzene Diazonium Salt and N_α,N_α-Bis(carboxymethyl)-L-lysine Hydrate for Assembly with Polyhistidine-Tagged Protein (RC)

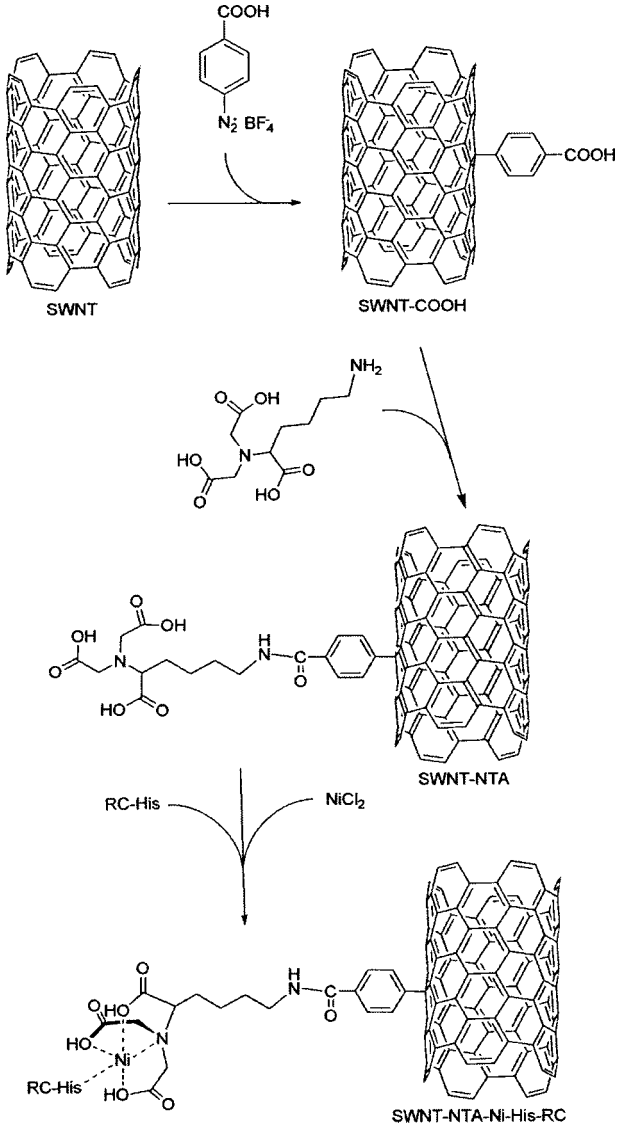

mM 4-carboxybenzene diazonium at 45 °C for 12 h. The diazonium concentration was then raised to 10 mM and reacted a second time at 45 °C for an additional 12 h to achieve a high extent of reaction. The functionalized nanotubes were flocked out of solution using 10 times excess of acetone, filtered, washed with acetone and methanol, and resuspended in DI water (pH 11) by bath sonication for 30 min, followed by benchtop centrifugation at 16 300*g* for 30 min. Raman scattering was used to assess the extent of reaction by tracking the relative changes in the D and G modes of the nanotubes. Atomic force microscopy was used to verify individual suspension of reacted nanotubes without surfactant.

SWNT-NTA. N_α,N_α-Bis(carboxymethyl)-L-lysine hydrate (NTA-NH_2) was dissolved in 12 mM phosphate buffered saline solution (PBS buffer, pH 8.3) at 3 mg/mL and mixed with SWNT-COOH at 11.44 mM NTA-NH_2, which is in excess of the original diazonium concentration, assuming that the majority reacted with the nanotube sidewall. The solution was left to react overnight at room temperature. Excess NTA-NH_2 was removed by dialysis against a NTA-NH_2-free Tris buffer (pH 7.4) with 10 000 MWCO dialysis tubing (Pierce). NTA-NH_2 has a molecular weight of 262.26 g/mol and should easily pass through the dialysis membrane. After 4 h, the buffer was switched out to allow further removal of unreacted N_α,N_α-bis(carboxymethyl)-L-lysine and repeated once more. The dialyzed sample was bath sonicated for 15 min to resuspend any aggregates. This resulting solution was analyzed with FTIR.

SWNT-NTA-Ni. The pH of the NTA-SWNT was adjusted to 11, and an equimolar amount of nickel chloride to NTA-NH_2 (before dialysis) was added to complex the nickel with the NTA at room temperature for 4 h. Not all NTA-NH_2 from the first reaction attached on the surface of the nanotube, but this concentration ensures an excess of nickel. The remaining nickel ions were removed by dialysis against Tris buffer at pH 7.4 using 10 000 MWCO dialysis tubing. The buffer was changed after equilibrating for 4 h and allowed to dialyze an additional 4 h and repeated once more. As a control a NTA-SWNT sample at pH 7 was also exposed to 10 μM Ni^{2+} and is expected to bind less nickel than the more alkaline solution at pH 11.

XPS was used for elemental analysis of the nickel complexed to the carbon nanotubes. XPS is a very sensitive surface technique so the nanotubes must be suspended in pure deionized water. To exchange the buffer, 1 mL of nickel-NTA-SWNT was dialyzed against 2 L of nanopure deionized water using dialysis tubing with a MWCO of 12 000–14 000 g/mol. The nanopure water was switched out two times to remove the remaining salt from the Tris Buffer after reaching equilibrium over 4 h.

SWNT-NTA-Ni-His-RC. The SWNT-NTA-Ni sample was functionalized with 1 μM His-tagged photosynthetic reaction centers (RC) in 0.5% lauryldimethylamine oxide (LDAO) surfactant, to maintain stability of the RC, and incubated overnight before imaging with the fluorescence microscope. His-tagged binding to functionalized carbon nanotube was reversed by adding 0.25 M imidazole to SWNT-NTA-Ni-His-RC complex. Control images were taken of 1 μM His-RC before and after the addition of 0.25 M imidazole as well as SWNT-COOH (no nickel) incubated with 1 μM RC-His to ensure that the RC-His binding is specific to the nickel on the nanotube surface. For near-infrared imaging with the fluorescence microscope glass slides were incubated in a solution of 12 mg/mL bovine serum albumin (BSA) to prevent adsorption of the protein complexes onto the glass slide. The slides were incubated for 10 min and then thoroughly rinsed with deionized water to remove excess BSA and dried with nitrogen. The RC samples were then deposited (10 μL) and sealed with a coverslip to prevent drying of the sample. Excess RC was removed from SWNT-NTA-Ni-His-RC using a nickel-chelated agarose resin (Qiagen). The sample was mixed with 2 times excess resin, incubated for 1 h, filtered through a 30 μm frit, and then rinsed with DI water (20% glycerol) with 0 mM imidazole (SA) and 10 mM imidazole (SB) to remove protein that is nonspecifically adsorbed to the resin and 0.5 M imidazole (EB) to elute RC from the resin. RC-His not bound to the nanotube will remain in the resin until eluted. This step was repeated until no RC is eluted from the resin with EB.

Analysis. *NMR.* ^{1}H NMR was performed with a Varian Unity 400 MHz spectrometer in deuterated acetonitrile.

Mass Spectroscopy. Measurements were performed with a Waters Q-Tof Ultima mass spectrometer using electrospray ionization to obtain a high-resolution mass spectrum after dissolving sample in water.

Raman Spectroscopy. Raman spectra were collected by back-scattering through a 10× objective by excitation with a 785 nm photodiode laser with a custom Kaiser Raman spectrometer.

AFM. Carbon nanotubes were deposited onto a silicon substrate coated with a monolayer of 3-aminopropyltriethoxysilane (APTES). The silicon wafer was cleaned with DI water, acetone, and isopropyl alcohol and then dried with nitrogen. The cleaned wafer was immersed in a solution of 1 M APTES for 10 min, rinsed with DI

water, and dried with nitrogen to create a monolayer of APTES. Carbon nanotubes were deposited on the wafer by soaking the substrate in a sample solution for 2–10 min, followed by rinsing with DI water and drying with nitrogen. AFM images of the deposited nanotubes were collected using a Nanoscope IIIa instrument in contact mode.

FTIR. Analysis was performed using a Thermo Nicolet Magna-IR 760 Spectrometer with a frequency range of 400–4000 cm^{-1}. Each measurement was based on eight scans with a 0.5 cm^{-1} resolution. Each sample was dried onto a Real Crystal IR sample card (KBr) from International Crystal Laboratories.

X-ray Photoelectron Spectroscopy (XPS). Measurements were performed using a Kratos Axis Ultra with an X-ray source from monochromatic Al, 1486.6 eV, 150 W (10 mM, 15 kV). The analysis area was 0.7 × 0.3 mm^2 in hybrid/slot mode with pass energy of 160 eV for survey measurements and 40 eV for high-resolution measurements while operating with the neutralizer on a floating stage. The C 1s binding energy for carbon nanotubes at 284.5 eV was used as a reference for the XPS features.

UV–Vis−NIR Absorption Spectroscopy. Absorption spectra were recorded with a double-beam Shimadzu UV-3101PC UV–Vis−NIR scanning spectrometer at a scanning rate of 200 nm/min through quartz cuvettes.

Fluorescence Microscopy. Fluorescent imaging was collected using an Axiovert 200 microscope (Zeiss) coupled to a 2-D InGaAs array detector (Roper Scientific) which detects fluorescence in the 800–1600 nm range. All samples were imaged with a 63× oil immersion objective using laser excitation at 785 nm from a photodiode laser (20 mW). Data were smoothed with a moving average over 5 pixels for the line mapping of fluorescence intensity to reduce noise.

Results and Discussion

Raman scattering of the surfactant-solubilized AP-SWNT (Figure 1A1) using a photodiode laser at 785 nm excitation showed a very small degree of defects in this starting material from the relative intensity of the D peak (1300 cm^{-1}) normalized to the G peak (1590 cm^{-1}). As the nanotubes react with the 4-carboxybenzene diazonium salt, the hybridization of carbon atoms changes from sp^2 to sp^3, increasing the number of defects in the nanotubes sidewall. Parts A2 and A3 of Figure 1 show a sizable increase in the disorder mode (1300 cm^{-1}) of the AP-SWNT during subsequent reaction to form SWNT-COOH as expected for sidewall functionalization of the carbon nanotubes from the 3 and 10 mM reactions, respectively. When the 10 mM reaction solution was flocked, washed, and resuspended in DI water (pH 11), the acid groups deprotonate, leaving the nanotube material water-soluble and stable. The relative extent of reaction (D/G ratio) was not significantly changed during the resuspension from the original reacted solution (Figure 1A4).

AFM images of the AP-SWNT suspended in 1% SDS (Figure 1B) show that the nanotubes before reaction are suspended in small bundles on the order of 7–8 nm in diameter after centrifugation (Figure 1C). The AFM images of SWNT-COOH (Figure 1D) without surfactant show nanotubes that are ∼3 nm in height, as seen in the height profile (Figure 1E), which is consistent with the sidewall addition to individual nanotubes. When the nanotubes are reacted with the 4-carboxybenzene diazonium, the diameters

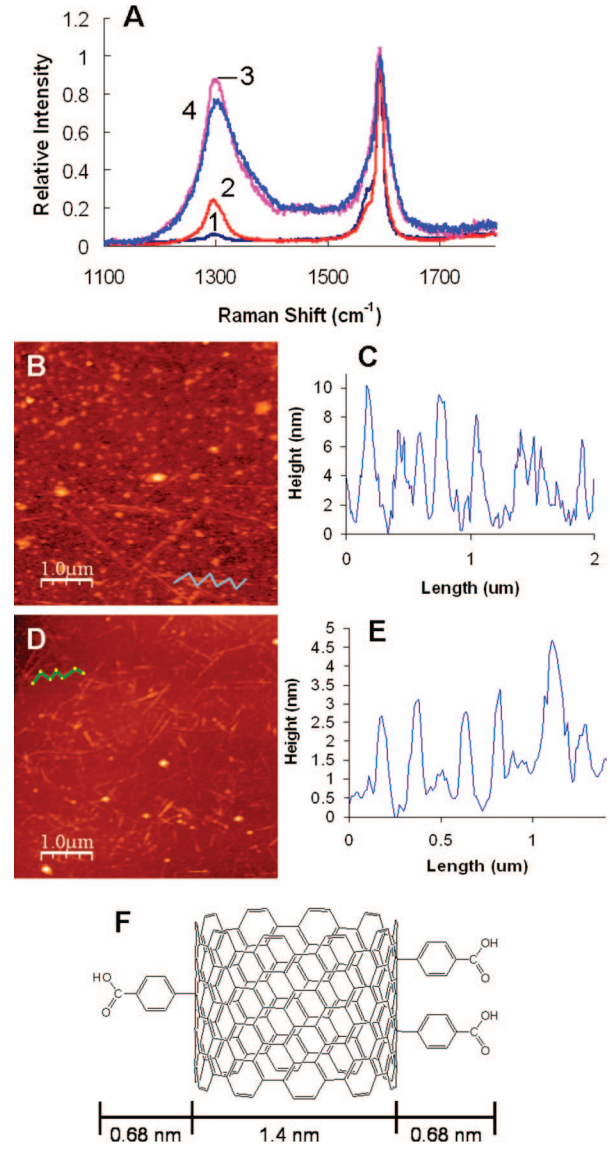

Figure 1. Raman scattering and AFM of SWNT functionalized with 4-carboxybenzene diazonium salt. (A) Increasing D mode (1300 cm^{-1}) with respect to G mode (1590 cm^{-1}) from starting material (1) to 3 mM (2) and 10 mM reaction (3). Resuspension of the reacted SWNT without surfactant (4) showed no significant change in the extent of reaction compared to the reacted SWNT in solution (3). (B) AFM of AP-SWNT in 1% SDS following centrifugation to remove large bundles. (C) Height profile of representative nanotube from AP-SWNT sample from figure B, showing nanotube bundles ∼7–8 nm in height. (D) AFM of SWNT-COOH after resuspension and centrifugation. (E) Height profile of representative nanotube from resuspended SWNT-COOH, showing reacted individual nanotubes ∼3 nm in height. (F) Length scale of SWNT-COOH reaction product. AP-SWNT have an average diameter of 1.4 nm; the sidewall addition adds 0.68 nm onto the nanotube radially, resulting in a diameter of 2.76 nm.

of individual nanotubes are expected to increase from 1.4 to ∼2.76 nm from the addition of the carboxyphenyl group to the nanotube sidewall, based on standard bond lengths (Figure 1F). If the 4-carboxybenzene diazonium reacted only on the outside of the bundles, we would expect to see a larger diameter in the reacted sample than in the starting material; however, the nanotubes are more stable individually with acid functionalization. Also, any large reacted bundles would be removed by the centrifugation during resuspension of the reacted nanotubes. We conclude that the sample contains individually suspended SWNT with carboxylic acid moieties decorating their surface after this step.

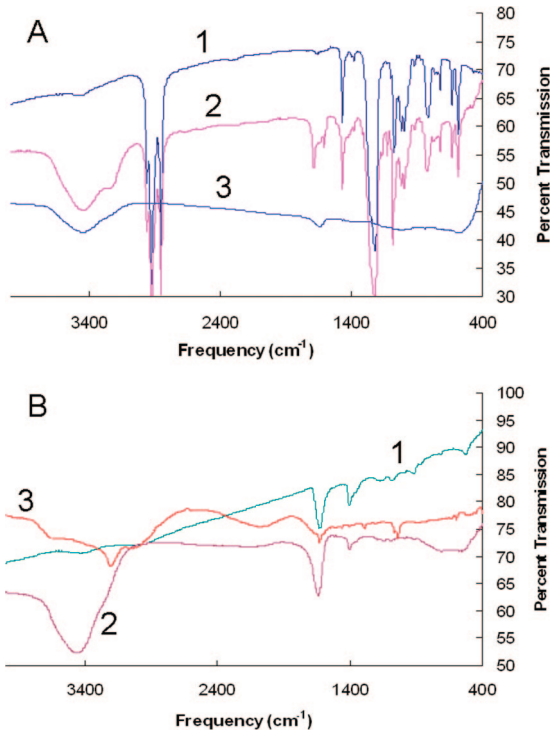

Figure 2. FTIR spectra. (A) (1) AP-SWNT in 1% SDS, peaks correspond to sodium dodecyl sulfate surfactant (SDS); (2) 10 mM reaction of AP-SWNT with O−H peak at ~3480 cm^{-1}, N−H peak at 3260 cm^{-1}, and a C═O peak at 1650 cm^{-1}; (3) resuspended reacted 10 mM SWNT-COOH without surfactant showing only C═O and O−H features as excess diazonium and surfactant has been fully removed. (B) (1) NTA-NH_2 in PBS buffer with O−H (3453 cm^{-1}), N−H (3030 cm^{-1}), C═O (1637 cm^{-1}), C−H (1405 cm^{-1}), and C−N (1205 cm^{-1}) peaks; (2) reaction solution of SWNT-COOH and NTA-NH_2 in PBS buffer, in addition to acid features there is also a peak at 1419 cm^{-1} corresponding to C−H bonds in the alkane chain of the NTA-NH_2; (3) dialyzed SWNT-NTA which have the O−H group (3583 cm^{-1}) from the NTA ligand as well as a N−H bond peak (3039 cm^{-1}), a C−N bond peak (1295 cm^{-1}), C−O peak (1041 cm^{-1}), and C═O (1633 cm^{-1}) as expected for SWNT-NTA formation.

FTIR measurements show carboxylic acid groups present in the reaction of SDS surfactant suspended AP-SWNT with 10 mM 4-carboxybenzene diazonium. The SDS suspended AP-SWNT have features that are dominated by the SDS surfactant at 400–1500 and 2900 cm^{-1} (Figure 2A1). The 10 mM reacted sample had an O−H peak at ~3480 cm^{-1}, a C═O peak at 1650 cm^{-1} from the acid groups on the surface of the nanotubes, and a peak at ~3260 cm^{-1} corresponding to N−H bond of unreacted or decayed diazonium salt in solution (Figure 2A2). FTIR analysis of the resuspended 10 mM SWNT-COOH after filtration and washing shows acid groups on the surface with peaks at 3480 cm^{-1} (O−H) and 1650 cm^{-1} (C═O) and no remaining peaks from the sodium dodecyl sulfate surfactant or from the unreacted diazonium (Figure 2A3).

N_α,N_α-Bis(carboxymethyl)-L-lysine hydrate (NTA-NH_2) has a nitrilotriacetic acid moiety as well as a primary amine on a short alkane chain. FTIR of NTA-NH_2 in PBS buffer has O−H (3453 cm^{-1}), N−H (3030 cm^{-1}), C═O (1637 cm^{-1}), C−H (1405 cm^{-1}), and C−N (1205 cm^{-1}) peaks as expected from the chemical structure (Figure 2B1). When reacted with SWNT-COOH, the resulting solution has a strong excess of NTA-NH_2, in addition to acid features there is also a peak at 1419 cm^{-1} corresponding to C−H bonds in the alkane chain of the NTA-NH_2 (Figure 2B2). Dialysis was used to remove the excess NTA-NH_2 and to analyze the chemical structure of the reaction product. In the formation of SWNT-NTA the amine moiety of N_α,N_α-bis(carboxymethyl)-L-lysine hydrate (NTA-NH_2) reacts with the carboxyl group on the SWNT by nucleophilic substitution, resulting in a new C−N bond (1295 cm^{-1}) which is present in the FTIR spectra of the resulting solution (Figure 2B3). SWNT-NTA product also had an N−H bond at 3039 cm^{-1} for the remaining N−H group on the NTA-NH_2 after forming an amide bond to the carboxylic acid group. The NTA-NH_2 has three acid groups that will complex with nickel which show C−O (1041 cm^{-1}), C═O (1633 cm^{-1}), and O−H (3583 cm^{-1}) bonds in the FTIR spectra as well. There is some aggregation of the SWNT-NTA during dialysis to remove the excess NTA-NH_2; the flocks can be redispersed with bath sonication, resulting in a stable solution of SWNT-NTA. We anticipate that colloidal stability may be increased by reducing the number of NTA groups per length of SWNT, and this will be explored in future work.

The pH of the SWNT-NTA was raised to 11 to allow for efficient complexation of nickel ions onto the NTA chelating groups under alkaline conditions. A sample was also complexed at pH 7 as a control. XPS measurements confirm the complexation of nickel onto SWNT-NTA at pH 11, while no nickel was present at pH 7. The nickel coverage on the pH 11 sample was 28.7 at. % nickel/carbon. Nickel complexation also leads to aggregation during dialysis which is resuspended with bath sonication.

Fluorescence imaging of RC alone (Figure 3B) showed that the RC is stable in solution and free of aggregates, and the fluorescence is a uniform signal from solution compared to a background without laser excitation (Figure 3A). SWNT-NTA-Ni-His-RC are visible in Figure 3C as the RC concentrates onto the surface of the nanotube, increasing the localized fluorescence intensity along the carbon nanotube. The average length of an AP nanotube is 2.5 μm, which is in agreement with the length scale of the concentrated RC-SWNT structures. This binding is specific for the nickel complexed to the surface as Figure 3D shows no binding of RC-His onto SWNT-COOH. Line maps of the intensity of the RC fluorescence in the NIR along the dashed lines in Figure 3A−D show significant signal from the RC complex above the background (Figure 3E). For the map of the RC-SWNT solution (3E3) there is a peak in fluorescence intensity at ~60 and 95 μm, which correspond to RC-SWNT structures in the line map at those locations, as the reaction centers concentrate onto the surface of the nanotube. The slight maxima in the line maps of the RC solutions correspond to the center of the laser excitation where the intensity of the excitation is the highest.

Separation of excess RC-His from RC bound to NTA-functionalized AP-SWNT was monitored by absorption of RC at 805 nm and verified with fluorescence imaging. Figure 4A plots the RC absorption at 805 nm of each of the elutions from the Ni-NTA-agarose column. RC-Ni-NTA-SWNT passed through the 30 μm frit during loading (L) of the sample leaving excess RC-His from solution bound to the resin. The RC-His does behave as expected during the

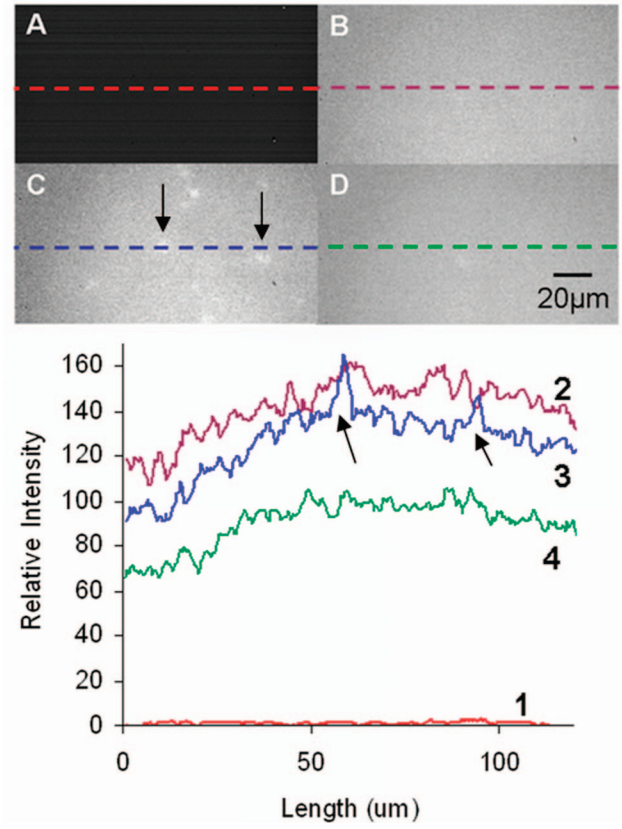

Figure 3. Near-infrared fluorescence imaging of RC complexes. (A) Background with no RC sample. (B) 1 μM RC-His which shows a uniform background fluorescence. (C) 1 μM RC-His bound to SWNT-NTA-Ni with bright spots where RC-His is densely covering the nanotube surface (complexes along dashed line marked with arrows). (D) 1 μM RC-His incubated with SWNT-COOH. The RC-His does not bind to the nanotubes in solution when nickel is not present. (E) Line maps of fluorescence along dashed lines in (A)−(D) with a moving average over 5 pixels in the image. (1) Background signal with no fluorescence, (2) 1 μM RC-His with uniform fluorescence from solution, (3) 1 μM RC-His bound to SWNT-NTA-Ni with a peaks at 60 and 95 μm corresponding to a RC-SWNT complexes (marked with arrows), and (4) 1 μM RC-His incubated with SWNT-COOH with uniform fluorescence from the RC without formation of RC-SWNT complex.

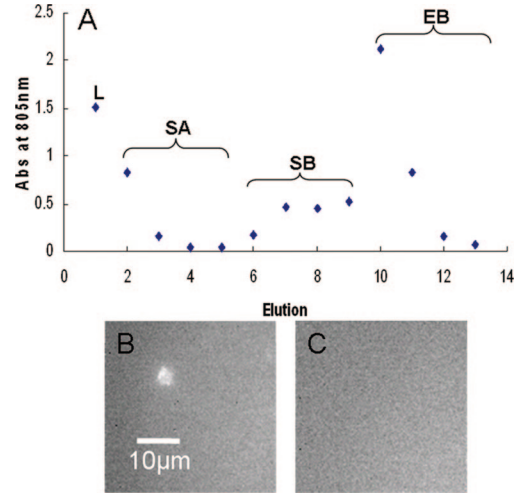

Figure 4. Separation of free RC from SWNT-NTA-Ni-His-RC. (A) Absorption peak of RC at 805 nm as the sample is eluted from a Ni-NTA-agarose resin to remove unbound RC from solution. (B) NIR fluorescent image of RC-Ni-NTA-SWNT separated into the loading sample (L) that passed through the frit. (C) Representative NIR fluorescent images of samples eluted with SA, SB, and EB, all showing uniform fluorescence of reaction centers without RC-SWNT structures.

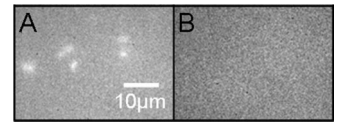

Figure 5. Reversibility of RC-His binding to SWNT-NTA-Ni. (A) 1 μM RC-His incubated with SWNT-NTA-Ni with RC concentrated onto the nanotube surface. (B) 1 μM RC-His on SWNT-NTA-Ni after addition of 0.25 M imidazole where RC binding has been redispersed into solution.

washing cycles as some RC comes out as imidazole is added at a low concentration (10 mM) with SB, while all the remaining RC elutes quickly for 0.5 M imidazole with EB. Each of these samples was imaged using the NIR fluorescence microscope to look for RC-Ni-NTA-SWNT structures which were only present in the loading sample (Figure 4B). Figure 4C is a representative image of the samples collected from elution with SA, SB, and EB with dispersed reaction centers unbound to carbon nanotubes.

The formation of the protein−nanotube complex by nickel−histidine binding was demonstrated through reversal with the addition of imidazole. Figure 5 shows NIR fluorescent images of SWNT-NTA-Ni-His-RC before (A) and after (B) the addition of 0.25 M imidazole. When imidazole is added to SWNT-NTA-Ni-His-RC, there is complete dissociation of the complex, resulting in resuspension of the RC and nanotubes into solution. The resulting near-infrared images of the RC bound to the functionalized nanotubes do show some signs of aggregation of the nanotubes into small bundles during synthesis; this will be the focus of a future study.

Conclusions

We have shown that single-walled carbon nanotubes can be covalently functionalized to bind nickel to the surface of the nanotube to direct the self-assembly of histidine-tagged proteins at controlled orientation. We have demonstrated that the histidine-tagged RC protein specifically binds to SWNT-NTA-Ni, that the free RC in solution can be removed though histidine binding to Ni-NTA-agarose resin, which can be removed by filtration, and that this binding on the nanotube is reversible. This approach has application for metal interacting protein systems where the redox center of the protein is inaccessible through conventional means of directed assembly onto carbon nanotubes.

Acknowledgment. This work was sponsored by the U.S. Department of Energy under the Solar Energy Initiative (Grant 104615). We thank Colin A. Wraight, Biochemistry Department at the University of Illinois at Urbana–Champaign, for supplying the polyhistidine-tagged photosynthetic reaction centers used in this study. The Q-Tof Ultima mass spectrometer was purchased in part with a grant from the National Science Foundation, Division of Biological Infrastructure (DBI-0100085). XPS measurements were carried out in the Center for Microanalysis of Materials, University of Illinois, which is partially supported by the U.S. Department of Energy under Grant DEFG02-91-ER45439.

CM702577H